Autoclaved Aerated Concrete – Limbachiya and Roberts (eds)
© 2005 Taylor & Francis Group, London, ISBN 0 415 38356 0

The most important aspects of microstructure influencing strength of AAC

G. Schober
Ing.-Büro für Material- und Verfahrenstechnik, Sägmühlstraße, Olching, Germany

ABSTRACT: AAC consists of pores by a volume fraction of 70 to more than 85%, depending on apparent density of the product. It is obvious that porosity is a major issue determining the properties of aircrete. A survey of all elements of microstructure will be given especially about those elements, which mostly affect the strength. Air pores make up the main part of pore volume in aircrete. Besides the typical ball like air pores some additional elements in pore structure are produced during expanding process. First of all there are small cracks often connecting the pores and showing a preferred orientation. The mineral composition of the solids skeleton, size, form and interconnection of the different crystals determine microstructure and resulting properties of the solid part of AAC. It is the amount of tobermorite, which provides high strength. But micro pore characteristics and mineral composition can vary and therefore result in a higher or lower strength.

1 INTRODUCTION

AAC is a material, which is produced in qualities with densities between 100 and 800 kg/m^3. There is no other industrial product that covers such a range in apparent density. Up from 350 kg/m^3 in apparent density AAC can be used as load bearing construction material. The material lower in density is used for thermal insulation purpose. No difference in production technology is needed to achieve this diversity. Only the part of pore volume produced by chemical reaction, in most cases aluminium powder is used, has to be adjusted. This way porosity is the most important microstructure element in AAC.

To provide you with an impression about the volume fractions of porosity and solid material in AAC products some examples for different density classes are listed in Table 1.

The material skeleton contains all the micro pores. Due to high total porosity skeleton material has to be in a rather optimized state in any way. There have to be a lot of very small tobermorite crystals,

Table 1. Porosity characteristics of AAC products different in density.

Apparent Density kg/m^3	Macro Pores %	Micro Pores* %	Total Porosity
100	83	13	0.96
150	77	17	0.94
350	70	16	0.86
400	65	19	0.84
600	45	~~21~~	0.76
800	27	41	0.68

* Total volume of micro pores is mainly controlled by water/solid ratio of raw materials mixture, thus it is possible to shift in a certain range from micro to macro pores and vice versa.

Erratum: 31

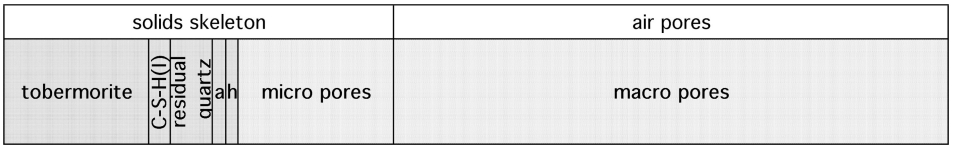

Figure 1. Schematic representation of volume parts in the structure of aircrete (a = anhydrite, h = hydrogarnet). Apparent density is about 400 kg/m^3 in this case, and raw materials are: pure quartz sand, lime, portland cement, anhydrite and water.

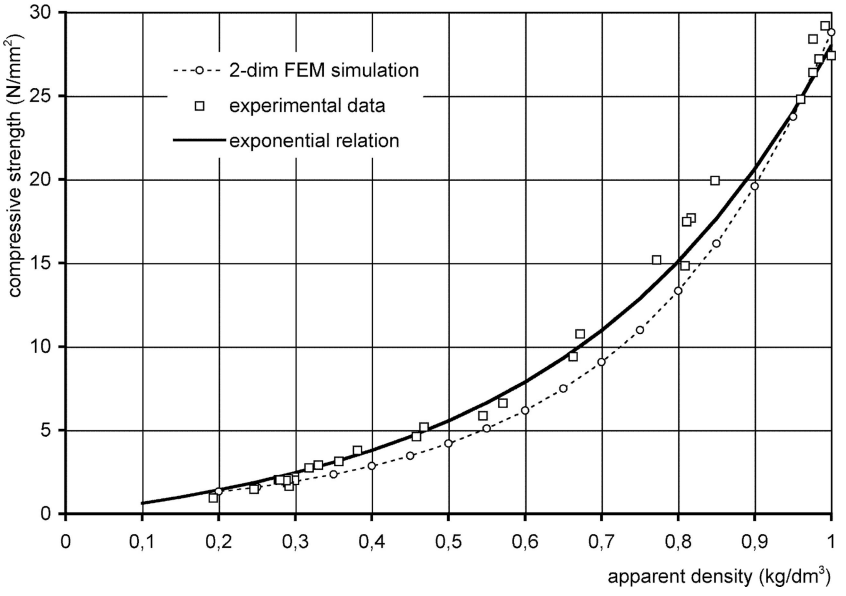

Figure 2. Relation between strength and apparent density of AAC over the range from 100 to 1000 kg/m^3.

well crystallized to create a binder which holds together all phases present. Besides tobermorite, which makes up between 50 to 80 vol.-% of solids one finds typically residual quartz and minor amounts of hydrogarnet and anhydrite. Figure 1 gives a representation of volume fractions of different microstructure components in AAC.

2 APPARENT DENSITY, MACRO PORE STRUCTURE AND STRENGTH

2.1 *Relation between strength and density*

An exponential law governs the relation between strength and apparent density. Over the range from 200 to 1000 kg/m^3 this has been proved by experiment and simulation.

The following expression was found to hold with a coefficient of determination of 0.99. It is a result from the simulation research work done in this field and from accompanying experiments (Schneider et al. 1998, Schneider 2001).

$$\sigma = \sigma_0 \times (\exp(3 \times D_{ap} \div D_{sk}) + D_{ap} \div D_{sk} - 1) \times \exp(-3) \quad (1)$$

where σ = compressive strength; σ_0 = compressive strength of not expanded but autoclaved material; D_{ap} = apparent density, D_{sk} = density of skeleton material.

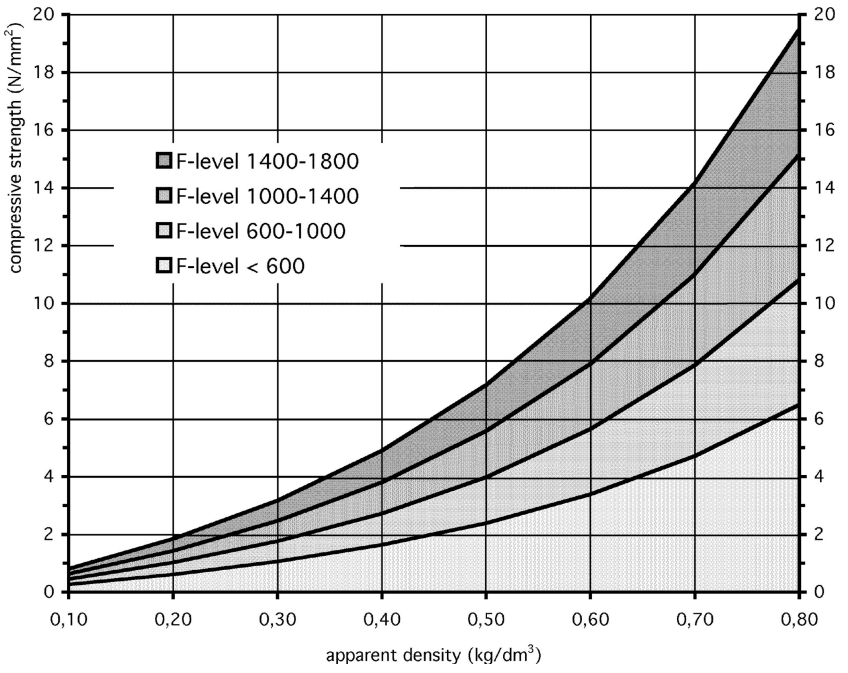

Figure 3. Strength density relations for AAC products, which differ in their quality levels. One curve represents one certain quality level in strength. These relations are also valid for foam concretes.

For different raw materials, properties of raw materials, formulations of AAC mixture and different autoclaving conditions one will get different curves. The following diagram shows a set of curves dividing the possible property combinations into quality classes.

If dry density values are not equal in one set of samples to be compared, it is possible to use this relation as a tool in quality control. A similar method is the so-called A-Zahl (A-value) widely used in Germany. But the A-value concept is only valid in the range from 400 to 750 kg/m^3. The figure of merit derived from the concept presented above may be called "strength level" or "F-level" and can be determined as follows when related to AAC:

$$F = \sigma \times 1000 \div (\exp(3 \times D_{ap}) + D_{ap} - 1) \tag{2}$$

where σ = compressive strength in N/mm^2; and D_{ap} = apparent density in kg/dm^3; it is assumed that σ_0 in equation (1) is about 21 N/mm^2 and D_{sk} around 1 kg/dm^3 respectively.

The "F-level" is a figure of merit for strength, which is independent of materials density.

In Figure 3 the possible property combinations are grouped into four classes of quality level regarding strength. One can use this to classify and compare raw materials situation and plant equipment conditions of different production sites for AAC.

2.2 *Anisotropy in strength of AAC*

It is a common known property of AAC that there is a difference in strength whether the load acts in rising direction or perpendicular to rising direction. This difference is not great but in some circumstances it is necessary to know about it. The following figure shows stress strain curves of two AAC samples out of the same lot, one compressed parallel to expanding direction and the other one compressed perpendicular to that direction.

The cause for this typical property of AAC has been found in a certain element of pore structure of the air pores. When the balls like air pores are generated, the slurry can move only in one

direction, upwards. At the end of this expanding process the viscosity of this foam gets so high that fission occurs in the pore walls. All this tiny cracks, which are finally connecting neighboring air pores, are orientated horizontically. This cracks all straightened are responsible for anisotropy in strength and in some other properties, see Figure 5.

The anisotropy in strength can range from 5 to 25%. It is around 10 to 15% in most of the AAC products. All influences, which affect viscosity of expanding mixture, can increase this anisotropy if viscosity runs too high at the end of expanding movements.

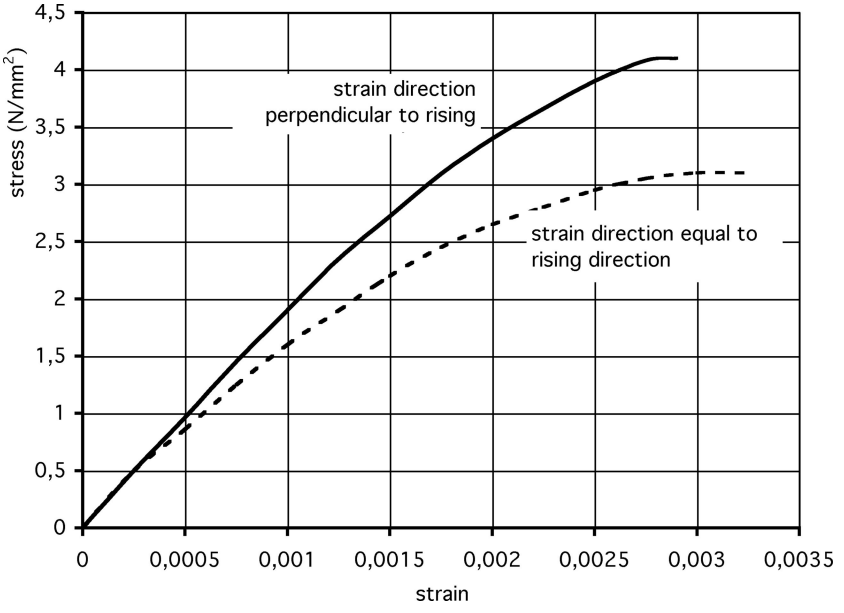

Figure 4. Stress strain relations of AAC cubes under compression in different directions relative to rising direction (expanding of the green cake).

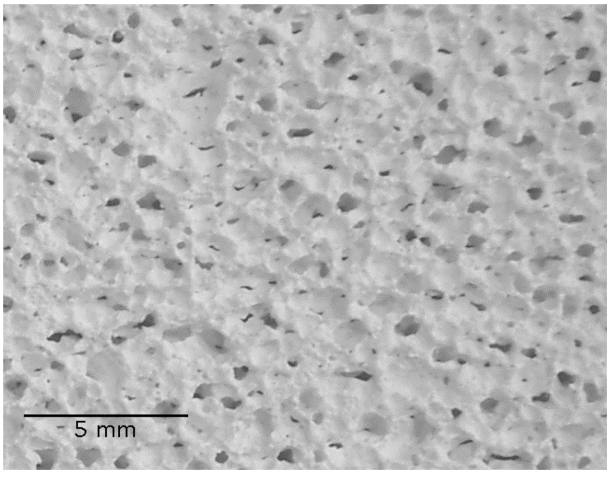

Figure 5. Photograph of AAC showing the micro crack structure produced during expanding process. Rising direction is from bottom to top, most cracks are orientated horizontically.

A suitable method to determine microstructure property related to micro cracks produced during expanding is measurement of gas permeability with respect to rising direction (Wägner et al. 1995).

Trials to avoid anisotropy in aircrete by using foam technology led surprisingly not to material without anisotropy. It turned out that the very small expansion due to temperature increase (lime and cement reactions) was sufficient enough to produce a similar effect as experienced with ordinary AAC making.

2.3 *Properties of pore size distribution of macro pores and their influence on strength*

The simulation of pore structures allowed to test a lot of characteristics of the pore size distribution of the air pores in AAC on their possible influence on strength.

The model in the simulation was a two-step one. Air pores were generated with certain properties of their size distribution, total porosity, minimum pore size, maximum pore size, minimum pore distance, mean pore size and type of size distribution. The solid part of the simulated pore structure was constructed by finite elements method (FEM). The solid material properties for FEM were Young's modulus, compressive strength and Poisson ratio. Additionally the solid part of the simulated pore structure was considered to be brittle and ruled by a Weibull distribution for its strength values. So another parameter the Weibull exponent (m) was included in this model. Most of the simulations were done on a two dimensional model. Details are described in Schneider et al. 1998 and Schneider 2001.

The results found in the simulation experiments can all be explained as effect of one single property of the air pores size distribution, and this is the minimum pore distance. In every case when two pores are very close together there exists a small volume element in the solid structure between these two pores, which comes under very high stress as soon as load acts on the sample. This volume element will be the weakest point in the structure and failure of the sample will start at this point.

As minimum pore distance is not independent of other pore structure properties the influence of mean pore size and broad or narrow size distribution in structures with the same porosity of air pores has been studied.

The influence of pore size proved to be directly proportional to strength as shown in Figure 6. This effect could be seen only when porosity was higher than 0.3. As soon as porosity is so high that the pores touch each other, this model doesn't hold any longer and therefore there is no answer in this case. The strength values as shown in Figure 6 can spread more or less according to minimum pore distance, which was allowed in the simulation runs. This does not change the positive trend for strength with pore size.

The character of pore size distribution turned out to be positive with respect to strength when it is a narrow one. Broad pore size distribution led to lower strength and also structures with a single pore size resulted in slightly lower strength than such with a narrow distribution of same mean pore size. These results too are only secondary effects of the minimal thickness of pore walls in the air pore structure of AAC.

3 SKELETON MATERIAL, PHASE COMPOSITION, MICRO PORES

3.1 *Solids*

The structure of the solid skeleton is made up by the binding material tobermorite as basic component. There is also a minor part of C-S-H(I) as a binder in most cases. All the CSH phases (Calcium-Silicate-Hydrate phases) in AAC are crystalline or semi-crystalline. No $Ca(OH)_2$ (portlandite) and C-S-H gel can be found in AAC of good quality.

The tobermorite crystals in AAC are very small in any case. What can be seen with SEM (scanning electron microscopy) always are only the biggest ones. Tobermorite forms during autoclaving and the crystals grow in form of laths, plates or bands. The single particles always crystallize with one

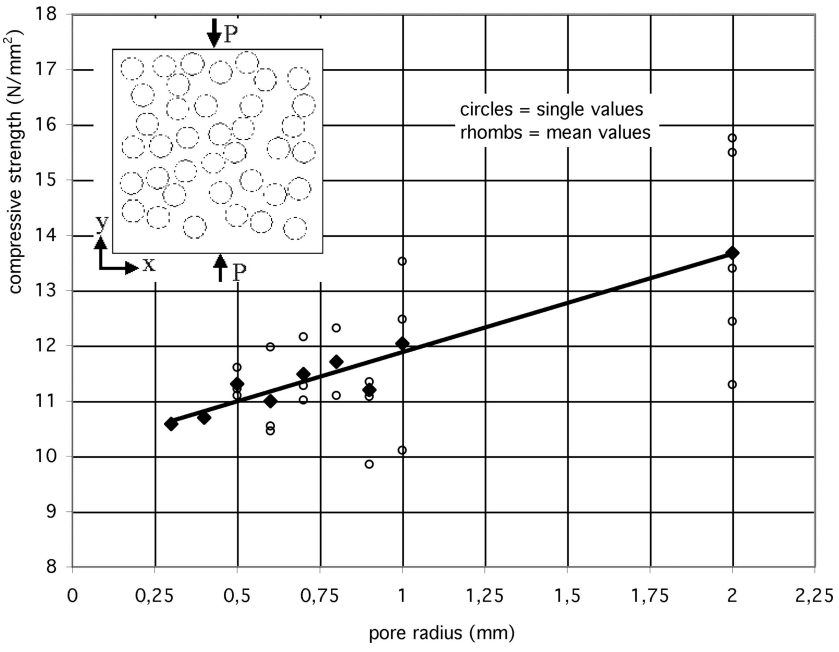

Figure 6. Strength of porous structures with different pore size of macro pores. Macro pore fraction is 0.4.

strongly preferred growing direction (silicate Dreierketten in the structure of tobermorite). Thus, intergrowing of these laths, plates or bands leads to the final strong microstructure, which becomes more and more dense during the autoclaving process.

There is no doubt that first of all the amount of tobermorite rules the strength of AAC products. All other components in AAC are incorporated in the tobermorite or C-S-H(I) mass. Figure 1 gives a schematic representation of the volume fractions for an example of AAC with 400 kg/m^3 in apparent density. Residual quartz, hydrogarnet and anhydrite are the typical accompanying phases in AAC. There may be some others according to which kind of raw materials are being used. If anyone of the minor components in AAC overruns about 10 to 15 mass-% strength will be reduced. This shows that none but CSH phases act as binder in AAC.

Formation of tobermorite microstructure is strongly influenced by raw materials, their properties and the autoclaving conditions. A major role concerning final strength are playing the intermediate sulphate phases, ettringite and hydroxylellestadite. The later acts as a precursor to tobermorite being formed in the final stage of autoclaving. Ettringite formation in the green cake seems to prepare the microstructure of the product, so that conditions for succeeding CSH intergrowing and reorganization of microstructure become more positive.

3.2 *Micro pores*

Most of the micro pores in AAC are remaining volume parts of space that first was occupied by water in the green cake and later on filled by reaction products. Only a small amount of the micro pores are new formed voids after dissolution of raw material particles e.g. quartz grains. Some of the residual quartz grains are not incorporated densely inside the CSH matrix. Quite often there can be found cavities around such quartz grains.

In the green cake mean pore size of micro pores is between 1 and 10 μm in diameter (Mitsuda et al. 1992). The final state after autoclaving shows mean pore sizes from 0.01 to 0.2 μm (Mitsuda

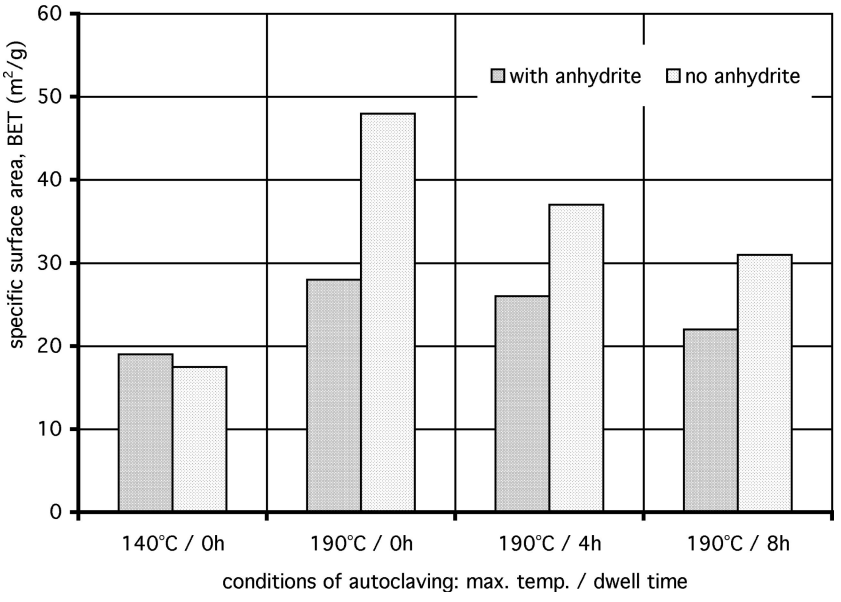

Figure 7. Specific surface areas of AAC autoclaved under different conditions. Results are given for two AAC sample series with different recipes, one with the other without anhydrite as a recipe component.

et al. 1992, Pospisil et al. 1992). In these cases measurement was done with mercury intrusion porosimetry method (MIP).

During autoclaving process, after a first CSH matrix has been formed with a maximum of frequency in pore size distribution lower than 0.1 μm, this maximum is going to shift slightly to somewhat higher values (Mitsuda et al. 1992). This effect is due to increase of tobermorite content. It means that the amount of crystalline CSH phases is growing and semi-crystalline CSH and intermediate reaction products are waning in the solid matrix. Determining the specific surface area with BET method shows this more clearly than MIP (Fig. 7). This change in microstructure is accompanied with an increase in strength.

What can be seen in Figure 7 as well is an effect of sulphates on microstructure. Anhydrite addition does not change the amount of CSH phases but it alters micro porosity. All the anhydrite added is present in the final product as anhydrite again, if autoclaving time was not too short. The positive effect on strength is due to formation of tobermorite in a way that leads to higher density of CSH matrix in AAC.

It is easy to change the amount of micro porosity in AAC by changing the water solid ratio (w/s) of the raw materials mixture. Such changes don't show a strong effect on strength. Trying to increase strength by reducing w/s results in higher viscosity of mixture and less stability of expanding process. Thus macro pore structure gets weakened and strength will be reduced.

4 DISCUSSION

An explanation to anisotropy in AAC that the air pores were egg shaped is still often told. But there is no evidence that the air pores are elliptical in shape and these ellipses would have a preferred orientation. The air pores are not all perfect spheres, but that is due to lack in space when the pores are almost touching each other. The only pores, which can be found with elliptical shape, are very large pores (entrapped air). They got their shape by streaming up some milli- or centimeters in the expanding slurry. If such pores were responsible for the difference in strength, then the effect would be the other way around, higher strength in rising direction and lower strength perpendicular to

rising direction. The real causes for anisotropy are the small cracks in the walls of the air pores. They are produced unavoidably during expanding process and their occurrence is strongly influenced by viscosity of mixture.

Concerning influence of air pore size on strength some authors report that big air pores lower strength and they try to confirm this with reference to Griffith theory (Pospisil et al. 1992). In this view the results presented in Section 2.3, Figure 6 seem to be in contradiction to Griffith theory. The theory deals with a single crack or hole in an infinite plate. In this imagined plate there exists no other weak point besides the one hole, the edge of which is acting as starting point of failure. Therefore it is obvious that aircrete can not be described by this theory unless there were very big isolated holes in the ordinary pore structure of AAC, and this holes then would have to be more than twenty times in size than the mean air pore size is.

The weakest point in the AAC structure is not at the edge of one of the biggest air pores, it is a section between two pores. Therefore notice, not pore size is decisive in this case but pore distance, i.e. the minimal thickness of pore walls. Only as a secondary effect pore size of air pores has an influence. If porosity is held constant then an increase in pore size results in thicker walls between the pores and so strength should be higher in pore structures with bigger pores. This effect should be valid if porosity due to air pores is higher than 0.35 but lower than in a state where the pores have to touch each other.

In phase composition tobermorite crystals have been found to be the only ones of a lot of possible CSH phases to bring to pass a binder matrix with high strength. So all raw materials and conditions, which don't support formation of well-crystallized tobermorite in AAC, are not advantageous. The knowledge on physical interaction between binder and minor components in AAC microstructure is rather poor.

Micro pores in AAC are mainly pores of nano-scale. These are connected to binder phase, the tobermorite crystal mass. The part, which could be active in capillary transport, is low. Increasing w/s strongly would produce more capillary pores but lower strength. With thermal insulation products based on CSH this is a common way of processing. But this is not done in AAC production. As reducing w/s is limited due to process engineering restrictions other methods to obtain a denser CSH matrix have to be tried. Until now, only the addition of sulphates is a method, which is known to work.

5 CONCLUSIONS

The microstructure of AAC can be improved with respect to getting a high strength by trying to achieve the following:

- an air pore structure with less cracks in the air pore walls as possible
- a size distribution for air pores, which is rather narrow
- air pores as big as possible, if the air pore porosity is within the range from 0.35 to 0.75
- amount of tobermorite in phase composition as high as necessary
- intergrowing of CSH matrix as dense as possible
- less micro pores due to dissolution of raw material particles, e.g. cavities around quartz

REFERENCES

Mitsuda, T., Kiribayashi, T., Sasaki, K. & Ishida, H. 1992. Influence of hydrothermal processing on the properties of autoclaved aerated concrete. In F. H. Wittmann (ed.), *Proceedings of the 3rd RILEM International Symposium on Autoclaved Aerated Concrete, Zürich, Switzerland, October 14–16 1992*: 11–18. Rotterdam: Balkema.

Pospisil, F., Jambor, J., Belko, J. 1992. Unit weight reduction of fly ash aerated concrete. In F. H. Wittmann (ed.), *Proceedings of the 3rd RILEM International Symposium on Autoclaved Aerated Concrete, Zürich, Switzerland, October 14–16 1992*: 43–50. Rotterdam: Balkema.

Schneider, T., Schober, G. & Greil, P. 1998. Numerical modeling of the strength of highly porous aerated autoclaved concrete. In Schwartz, D.S. & Shih, D.S. & Evans, A.G. & Wadley, H.N.G. (eds), *Proceedings of the Materials Research Society, Vol. 521, San Francisco, California, USA, April 13–15 1998*: 21–26. USA: MRS Warrendale.

Schneider, T. 2001. Modellierung der Festigkeit poröser Keramiken. Dissertation, Technische Fakultät der Universität Erlangen-Nürnberg, Berlin: Logos Verlag.

Wägner, F., Schober, G., Mörtel, H. 1995. Measurement of gas permeability of autoclaved aerated concrete in conjunction with its physical properties, *Cement and Concrete Research* 25: 1621–1626.